J. Phys. F: Metal Phys., 11(1981)623–39. Printed in Great Britain

Pressure and temperature dependence of electrical resistivity of Pb and Sn from 1–300 K and 0–10 GPa—use as continuous resistive pressure monitor accurate over wide temperature range; superconductivity under pressure in Pb, Sn, and In

A Eiling and J S Schilling
Institut für Experimentalphysik IV, Universität Bochum, D-4630 Bochum, Germany

Received 2 June 1980, in final form 20 October 1980

Abstract. The dependence of the electrical resistivity of Pb on hydrostatic pressure is determined over major portions of the temperature and pressure ranges 1–300 K and 0–10 GPa (100 kbar), respectively, and for Sn at 300 K. The results are compared to a simple Bloch–Grüneisen law including volume changes due to thermal contraction. It is demonstrated that both Pb and Sn are ideally suited for use as accurate resistive manometers, enabling a reliable continuous determination of pressure over a wide temperature range. The agreement between the pressure at low temperatures indicated by both resistive and superconducting (T_c) Pb manometers is excellent. $T_c(P)$ calibration curves are given to 22 GPa for Pb and to 5 GPa for Sn and In. A general method is presented which shows how pressure can be used to test for the presence of electron–electron scattering; in the temperature range studied, $T \geqslant 7.2$ K, electron–phonon scattering constitutes the dominant scattering mechanism in Pb, as expected.

1. Introduction

The temperature dependence of the resistivity of a metal $\rho(T)$ contains a wealth of information about its electronic, magnetic and lattice states. Detailed comparisons between experiment and theory are, however, complicated by the fact that variation of the temperature invariably leads to changes in sample volume due to thermal expansion. Studies of the dependence of the resistivity on hydrostatic pressure are of interest in this regard because they reveal its full functional dependence on the two independent variables temperature and pressure $\rho(T, P)$, allowing not only a correction of the measured temperature dependences to constant volume but also a determination of the dependence of the resistivity on a second thermodynamic variable, namely pressure. We present here the results of hydrostatic pressure resistivity studies on elemental Pb from 1–300 K and 0–10 GPa (1 GPa ≡ 10 kbar) and Sn at 300 K from 0–10 GPa. Above 40 K the resistivity of Pb, $\rho(T, P)$, can be accurately fitted using a Bloch–Grüneisen expression with only two free parameters. The pressure scale at ambient temperatures is defined by well known structural phase transitions of Bi and Tl.

0305-4608/81/030623 + 17$01.50

A second more applied motivation for an accurate determination of $\rho(T, P)$ for Pb and Sn is to establish their usefulness as secondary resistive manometers accurate over a wide temperature and pressure range. A determination of the pressure at all temperatures is of interest because in the majority of pressure cell designs the pressure changes continuously with temperature.

Pb and Sn are particularly suitable candidates for use as 'resistive manometers' because of their wide use as low-temperature superconducting manometers. Their superconducting transition temperatures decrease sensitively with pressure (Clark and Smith 1978, Eichler and Wittig 1968, Wittig *et al* 1979). It will be shown, in fact, that the resistivity $\rho(T, P)$ manometer can be used to check and extend the calibration range of the superconducting $T_c(P)$ manometer. The development of such continuous pressure monitors, accurate over wide pressure and temperature ranges, serves to increase the usefulness of the high-pressure method in quantitative studies of the properties of matter.

In all metals at sufficiently high temperatures the dominant contribution to the temperature dependence of the resistivity originates from electron–phonon scattering ρ_{ep}. It is widely believed that at sufficiently low temperatures a second mechanism, namely the electron–electron scattering ρ_{ee}, becomes dominant (Ziman 1972, Lawrence and Wilkins 1973). One method of identifying ρ_{ee} in simple sp metals, for instance, is to search for its characteristic temperature dependence $\rho_{ee} \propto T^2$, as opposed to the expected dependence $\rho_{ep} \propto T^5$ at sufficiently low temperatures. We would like to propose an additional means of establishing the relative importance of the electron–electron scattering, namely, by measuring the pressure dependence of the temperature-dependent part of the resistivity. It will be shown that because of the rapid increase of the Debye temperature with pressure in Pb, for a given temperature dependence ρ_{ep} should decrease several times more rapidly than ρ_{ee}. Our studies indicate that for Pb the electron–phonon scattering dominates at all temperatures above $T_c = 7.2$ K, as would be expected (Lawrence and Wilkins 1973). The present method is, however, applicable to studies on arbitrary systems at lower temperatures and would complement the traditional temperature-dependence studies.

2. Experimental procedure

The present experiments were carried out using a recently developed hydrostatic pressure cell to 10 GPa suitable for precise electrical and magnetic measurements to low temperatures (Fasol and Schilling 1978, Eiling and Schilling 1979). The actual pressure chamber consists of a 2 mm diameter bore in a steel gasket filled with a 4:1 mixture of methanol and ethanol. Two opposed WC anvils are pressed into the metal gasket by a 30 ton six-bolt pressure clamp (Zimmer 1977), thereby reducing the cell volume and generating pressure in the fluid. The methanol–ethanol mixture remains fluid to 10 GPa at 300 K, passing through a glass transition at higher pressure (Piermarini *et al* 1978).

High-accuracy four-point DC resistivity measurements under pressure can be carried out on two samples simultaneously. The sample dimensions are approximately 0.8 mm × 0.3 mm × 0.1 mm with 0.3 mm sideways protrusions to which 26 micron diameter copper voltage contacts are spot welded. The resolution of the measuring apparatus is about 1 nV with $1:10^4$ relative accuracy. The temperature is determined using calibrated Ge and Pt thermometers. See a previous publication for more details

(Schilling *et al* 1976). The superconducting transition temperatures can be measured either resistively or using an AC inductance technique with miniature (1 mm outer diameter, 0.3 mm inner diameter) primary and secondary coils.

The polycrystalline samples measured are cut from 99.999% pure Pb, Bi and Sn (Demetron, Hanau) and 99.95% pure Tl (Riedel de Haen). All samples were measured in the as-received condition.

3. Results and analysis

3.1. Dependence of resistivity on temperature and pressure

We first discuss the determination of the pressure dependence of the resistivity of Pb and Sn at room temperature using well known transition points of Bi and Tl. The samples Pb and Bi, Pb and Tl, and Pb and Sn were measured pairwise together in three separate pressure cells. In figure 1 the relative resistances of Bi and Tl are plotted versus the relative resistance of Pb for increasing and decreasing pressure. The purely hydrostatic pressure conditions across the entire pressure range result in sharp phase

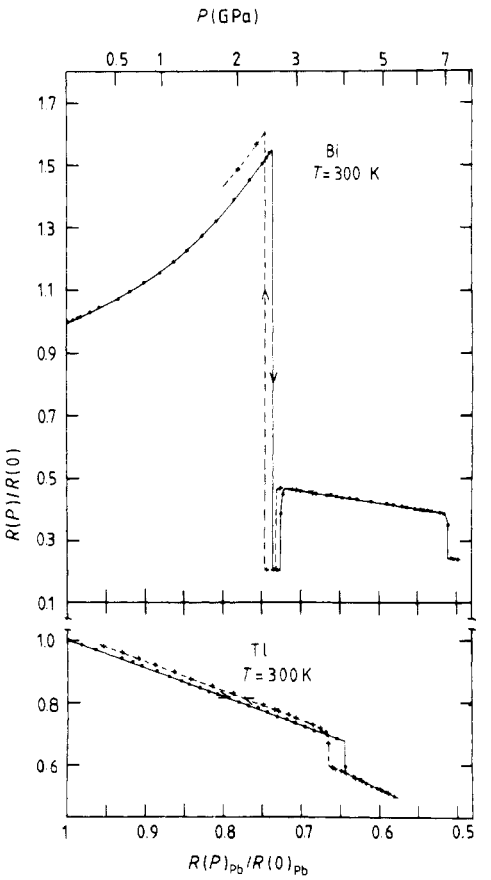

Figure 1. Relative resistance of Bi and Tl at 300 K versus relative resistance of Pb for decreasing and increasing pressure. Upper pressure scale derived from figure 2.

Table 1. Calibration pressure for relative resistance of Pb at 300 K. Error estimate in the resistance gives width of the hysteresis (see figures 1 and 2).

Transition	P (GPa)	$(R(P)/R(0))_{Pb}$
Bi I–II	2.55 ± 0.006[a]	0.739 ± 0.004
Bi II–III	2.69 ± 0.005[b]	0.726 ± 0.004
Tl II–III	3.67 ± 0.05[a]	0.654 ± 0.01
Bi III–V	7.3 ± 0.2[c]	0.508 ± 0.005

[a] Decker *et al* (1972).
[b] Zeto and Vanfleet (1969).
[c] Homan (1975).

transitions. The pressure dependence of the resistivity of Bi and Tl is in reasonable agreement with previous measurements by Bridgman and Bundy (see Bundy and Strong 1962). The midpoint of the pressure hysteresis for the Bi I–II, Bi II–III, and Tl II–III transitions defines the calibration points for our Pb resistance scale. The pressure at the midpoint of the transition is taken to define the Bi III–V transition which was only measured with increasing pressure. These results are summarised in table 1. In figure 2 the relative resistance of Pb and Sn is plotted versus pressure using the calibration points from table 1 and including previous studies by Bridgman (Landolt Börnstein 1960). A further study by Bundy and Strong (1962) for Pb lies considerably below the above data and is not included in figure 2. The full curves in figure 2

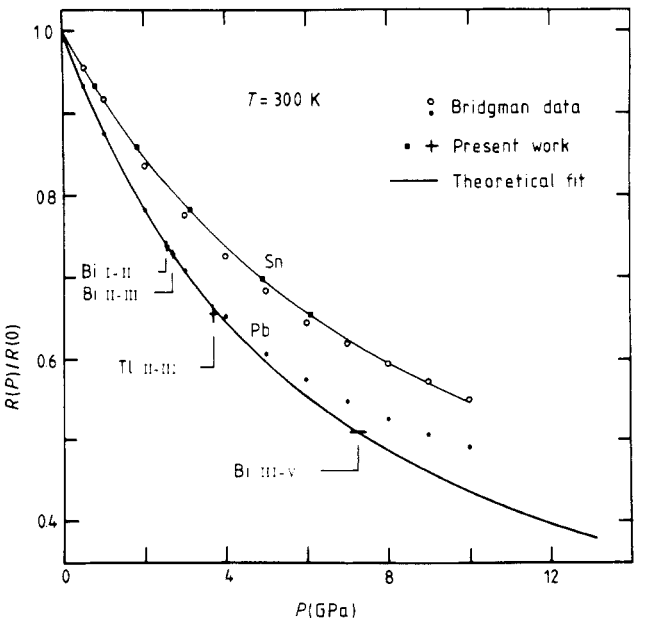

Figure 2. Relative resistance of Pb (+) and Sn (■) versus pressure at 300 K. Pb resistance is calibrated directly using data in table 1. Vertical 'error bars' give the magnitude of hysteresis seen in figure 1. Sn resistance is calibrated versus Pb resistance. The data of Bridgman (Landolt Börnstein 1960) are given by circles (○) for Sn and dots (●) for Pb. The full curve gives the fit using equations (4), (5) and (6) and table 2 for pressures below 13 GPa (Pb) and 10 GPa (Sn) where phase transitions occur.

are derived from a one-parameter theoretical fit which will be described in detail below. The agreement between the theoretical curves and the calibration points is generally excellent for both Pb and Sn.

As the basic approximate description of the pressure and temperature dependence of the electrical resistivity we use the standard Bloch–Grüneisen law which gives the resistivity contribution from electron–phonon scattering in the Debye limit, neglecting the Umklapp processes (Ziman 1972):

$$\rho_{BG}(T, P) = \frac{K}{\theta}\left(\frac{T}{\theta}\right)^5 \int_0^{\theta/T} \frac{z^5 e^z dz}{(e^z - 1)^2} \tag{1}$$

where θ is the Debye temperature and in K we combine together factors depending on the details of the Fermi surface geometry and scattering matrix elements. Note that K is independent of θ. Equation (1) is of the form $\rho_{BG}(T, P) = (K/T)f(T/\theta)$; including contributions from Umklapp processes, which are very important in polyvalent metals like Pb and Sn (Lawrence and Wilkins 1973), will change the form of $f(T/\theta)$, but not its functional dependence on the ratio T/θ. It thus follows from equation (1) that one can write (Dugdale 1969):

$$\frac{\partial \ln \rho_{BG}}{\partial \ln V} = \frac{\partial \ln K}{\partial \ln V} + \gamma\left(1 + \frac{\partial \ln \rho_{BG}}{\partial \ln T}\right) \tag{2}$$

where V is the sample volume and $\gamma = -(\partial \ln \theta/\partial \ln V)$ is the lattice Grüneisen constant. At sufficiently high temperatures ($T > 2\theta$) equation (1) reduces to $\rho_{BG} = (KT/4\theta^2)$ so that using equation (2) one obtains

$$\frac{\partial \ln \rho_{BG}}{\partial \ln V} = \frac{\partial \ln K}{\partial \ln V} + 2\gamma. \tag{3}$$

The pressure dependence of the resistivity can thus be broken up into two parts, the first term giving the changes under pressure of the Fermi surface geometry and electron–phonon matrix elements, and the second positive term describing the extent to which the phonon system entropy is lowered by pressure (lattice stiffening or shift of the phonon spectrum to higher frequencies). To calculate $\partial \ln \rho_{BG}/\partial \ln V$ from figure 2 a relation between sample volume and applied pressure P is required. To get this relationship we use the Murnaghan equation of state

$$V/V_0 = \left(\frac{PB'}{B} + 1\right)^{-1/B'}. \tag{4}$$

For B and B' we took the values of Mao given in table 2 (see Bassett and Takahashi 1974). These values are in good agreement with those given by Vaidya and Kennedy (1970). From the initial pressure dependence of the resistivity of Pb we obtain at 300 K, $\partial \ln \rho_{BG}/\partial \ln V \simeq +6.13$. Since $\gamma = \gamma_0 = +2.629$ at low pressures (Boehler *et al* 1978), we obtain from equation (3) $\partial \ln K/\partial \ln V = +0.87$. Similarly for Sn we derive, since $\gamma = \gamma_0 = +2.1$ (see Gschneider 1964), $\partial \ln K/\partial \ln V = +0.78$. In both Pb and Sn, therefore, the decrease of the resistivity with pressure originates predominantly from the 2γ or 'lattice stiffening' term in equation (3). At temperatures below 300 K this second term is even more dominant because $\partial \ln \rho_{BG}/\partial \ln T$ becomes more positive.

Table 2. Parameters used in the calculation of temperature and pressure dependence of the resistivity. Symbols are defined in the text.

Metal \ Parameters	θ_0 (K)	γ_0	B (GPa)	B'	K_0 (K^{-1} cm Ω)	β	δ	α ($\times 10^{-6}$ K^{-1})	C	η
Pb	86[a]	2.629[b]	43.7[c]	0.44[c]	2091[f]	0.87[g]	1.2[b]	28.9[a]	0.55[g]	6.5[d]
Sn	210[a]	2.1[a]	55.81[c]	0.27152[c]	7440[f]	0.78[g]	1.8[g]	21.2[a]	0.70[h]	7.0[d]

[a] Gschneider (1964).
[b] Boehler *et al* (1978).
[c] Bassett and Takahashi (1974).
[d] Fitted to the data of Bridgman (1970).
[e] Vaidya and Kennedy (1970).
[f] Landolt Börnstein (1960).
[g] Fitted to present data.
[h] Fitted to data from Washburn (1929).

In order to calculate the theoretical curve in figure 2 we use a more accurate expansion of equation (1) given by

$$\rho_{BG}(T, P) = \frac{KT}{4\theta^2}\left[1 - \frac{1}{18}\left(\frac{\theta}{T}\right)^2 + \frac{1}{480}\left(\frac{\theta}{T}\right)^4\right]. \tag{5}$$

This expression, in fact, agrees with equation (1) to within 0.6% for $T \geqslant (1/2)\theta$. A lower order series expansion was used by Moore and Graves (1967). Furthermore, it is important to take into account the pressure (volume) dependences of K, θ and γ using the following expressions

$$K = K_0(V/V_0)^{\beta} \qquad \theta = \theta_0(V/V_0)^{-\gamma} \qquad \gamma = \gamma_0(V/V_0)^{\delta}. \tag{6}$$

Values of the parameters for equation (6) are given in table 2. The only free parameter in the theoretical fit in figure 2 using equation (5) is the value $\partial \ln K/\partial \ln V = \beta$. The agreement between the theoretical curve from this simple Bloch–Grüneisen expression and the experimental calibration points in figure 2 is seen to be excellent. For Pb the data have been extrapolated beyond the last calibration point at 7.3 GPa to 13 GPa; it should be emphasised that this extrapolation is only as good as the accuracy to these high pressures of the above volume dependences of the various parameters. Future work will surely correct these values somewhat, necessitating a re-evaluation of the pressure dependence of the resistivity above 8 GPa.

Parallel to the above room-temperature studies we carried out measurements of the temperature dependence of the resistivity of Pb from 300–7 K on hydrostatic pressure to 4.4 GPa. In figure 3 we compare our $P = 0$ measurements to previous studies (Moore and Graves 1973, Van den Berg 1948). Included in this figure are a Bloch–Grüneisen fit using equations (1), (5) and (6) and table 2, and a first principles calculation by Tomlinson and Carbotte (1977). In the fit using equations (1), (5) and (6) and table 2 the decrease in sample volume upon reducing the temperature is taken into account using the following expression for the pressure-dependent thermal expansion coefficient (Birch 1952, Bridgman 1970):

$$\alpha = \alpha_0\left(1 - \eta\frac{P}{B}\right). \tag{7}$$

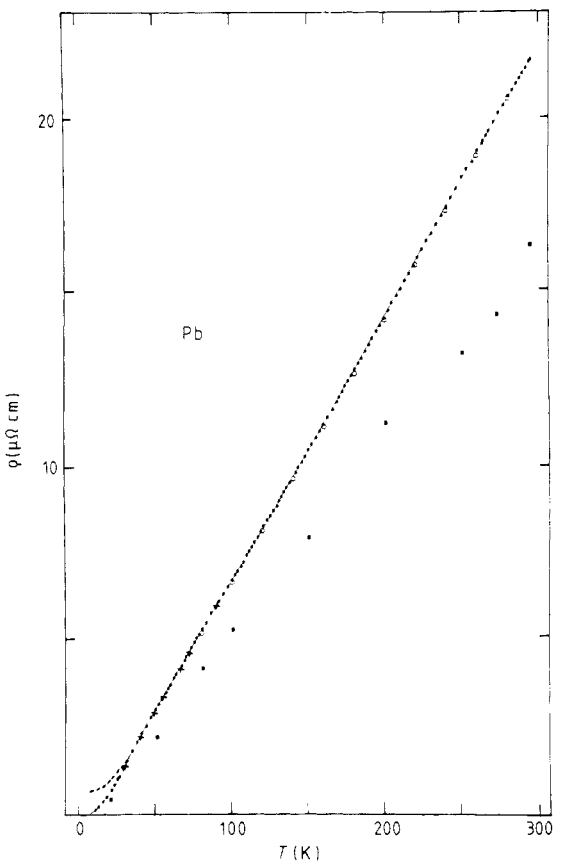

Figure 3. Measured resistivity of Pb at ambient pressures compared to the semiempirical formula in equations (1), (6) and (8) and table 2 (——) and equations (5), (6) and (8) and table 2 (– – –). The deviation of the latter high-temperature expansion (– – –) is clearly seen at temperatures below 30 K. Measurements of Van den Berg (1948) (+), Moore and Graves (1973) (○), present results (●), and calculations of Tomlinson and Carbotte (1977) (■).

The value of η was determined by fitting the data of Bridgman at low pressures. Using for the total volume change the product of that from the Murnaghan equation (4) and that from the thermal contraction, we obtain

$$\frac{V}{V_0} = [1 - 3C\,\alpha(300\,\mathrm{K} - T)]\left[\left(\frac{PB'}{B} + 1\right)^{-1/B'}\right] \tag{8}$$

where C is a fit parameter. The same procedure has been carried out for Sn using published ambient pressure data (Washburn 1929); the values of the parameters are again given in table 2. The fact that equation (5) provides such excellent fits to the data for Pb and Sn, both for the pressure dependence at 300 K and the temperature dependence for Pb and Sn at $P = 0$, using only two adjustable parameters, C and β, seems remarkable considering the crudeness of the approximations involved. In particular the Umklapp scattering is certainly expected to be very significant for both Pb

and Sn over our temperature range (Lawrence and Wilkins 1973). We also plot in figure 3 the full Bloch–Grüneisen expression in equation (1) using the same values of the parameters as above. Below 40 K the quality of the fit is much improved, although, as will be discussed in full below, the fit is still far less satisfactory than for $T > 40$ K.

We now make further assumptions, in view of the success of the above data fits, that equations (5)–(8) and table 2, including the appropriate volume dependences of the parameters, give a reliable description of the resistivity of Pb over the *entire range of temperature* 40–300 K *and pressure* 0–10 GPa (for Sn the corresponding ranges are 100–300 K and 0–10 GPa). In figure 4 we plot the temperature dependence of the resistivity at different pressures for Pb using equation (5). By comparing experimental high-pressure data to these isobars it is possible to estimate how much the pressure changes as the experimental apparatus is cooled down. We consider such an application in the following section.

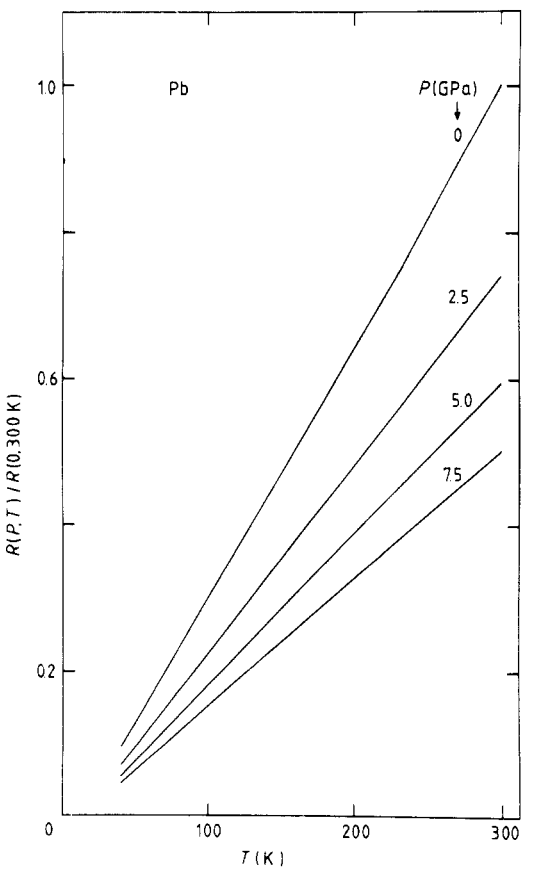

Figure 4. Plot of the theoretical temperature dependence of the relative resistance at different pressures from equations (5)–(8) and table 2.

3.2. Pb and Sn: resistive and superconducting manometers

In the preceding section we have derived a simple Bloch–Grüneisen expression for the resistivity of Pb, $\rho_{BG}(T, P)$, given by equations (5)–(8) with the values of the parameters in table 2 which should be accurate to a few per cent over the ranges 40–300 K and 0–10 GPa. In particular, one can calculate the resistivity isobars as a function of temperature. In many low-temperature high-pressure systems, the pressure is set at room temperature before the apparatus is cooled down to helium temperatures. The above isobars give a nominal value of the resistivity at all temperatures and thus allow an accurate determination not only of the pressure applied at room temperature, but also of the possible changes of this pressure as the temperature is lowered. Pb, and also Sn, can thus act as accurate continuous manometers over a wide temperature and pressure range! In quantitative studies of matter under pressure it is of the utmost importance to know both the pressure and temperature accurately over the entire range of the parameters. Pb and Sn are particularly useful as resistive manometers because they have long been widely used as superconducting manometers in the very low-temperature range. Incorporating two kinds of manometer, resistive and superconducting, into a single probe also allows a particularly direct calibration of one against the other, serving as a consistency check of the assumptions made in determining the calibration values of both.

In figure 5(*a*) we plot the resistivity of Pb versus temperature for four different room-temperature pressures 0, 0.8, 2.6 and 4.1 GPa. The Pb sample is mounted in the metal-gasket-type hydrostatic pressure cell. The theoretical isobars from equation (5) are drawn in as full lines. With the exception of the $P = 0$ measurement, which occurs at constant pressure, the data are seen to lie *below* the isobars for temperatures below 300 K. Since, at a given temperature, the resistivity of Pb decreases under pressure for $P < 13$ GPa, the immediate conclusion is that in the metal-gasket pressure cell the pressure increases with decreasing temperature. This pressure increase can be estimated by using the relation

$$\Delta P = (\rho_{exp} - \rho_{BG})\,(\Delta P/\Delta\rho)\,|_T \tag{9}$$

where $(\Delta P/\Delta\rho)_T$ is calculated from equation (5). This derivative is shown in figure 6 as a function of the temperature at various pressures. Using equation (9) it is thus possible to compute the pressure change ΔP as a function of temperature, as shown in figures 5(*b*) and 5(*c*). A measure of the accuracy of the method is given by its application to the $P = 0$ curve where the pressure is independent of temperature; the indicated pressure variation here, ± 0.1 GPa, simply reflects the quality of the fit of the Bloch–Grüneisen expression in equation (5) to the data. Note the larger error at low temperatures which is a consequence of the increase in $-(\Delta P/\Delta\rho)_T$. At high pressures as seen in figure 5(*b*), the pressure no longer remains constant, but rises with decreasing temperature and passes through a broad maximum at 100 K. The initial pressure rise is believed to originate from an approximate 25% increase in the applied force upon cooling down from 300 to 100 K. At 100 K this force increase apparently saturates, allowing the thermal contraction of the pressure fluid to dominate which decreases the pressure. For $T \lesssim 40$ K, the thermal contraction is expected to have saturated and no further pressure changes should occur. The fact that $\rho_{BG}(T, P)$ in equation (1) or equation (5) is unable to fit accurately even isobaric data for $T \leqslant 40$ K is thus of no consequence for the use of Pb as a resistive manometer over the entire temperature range.

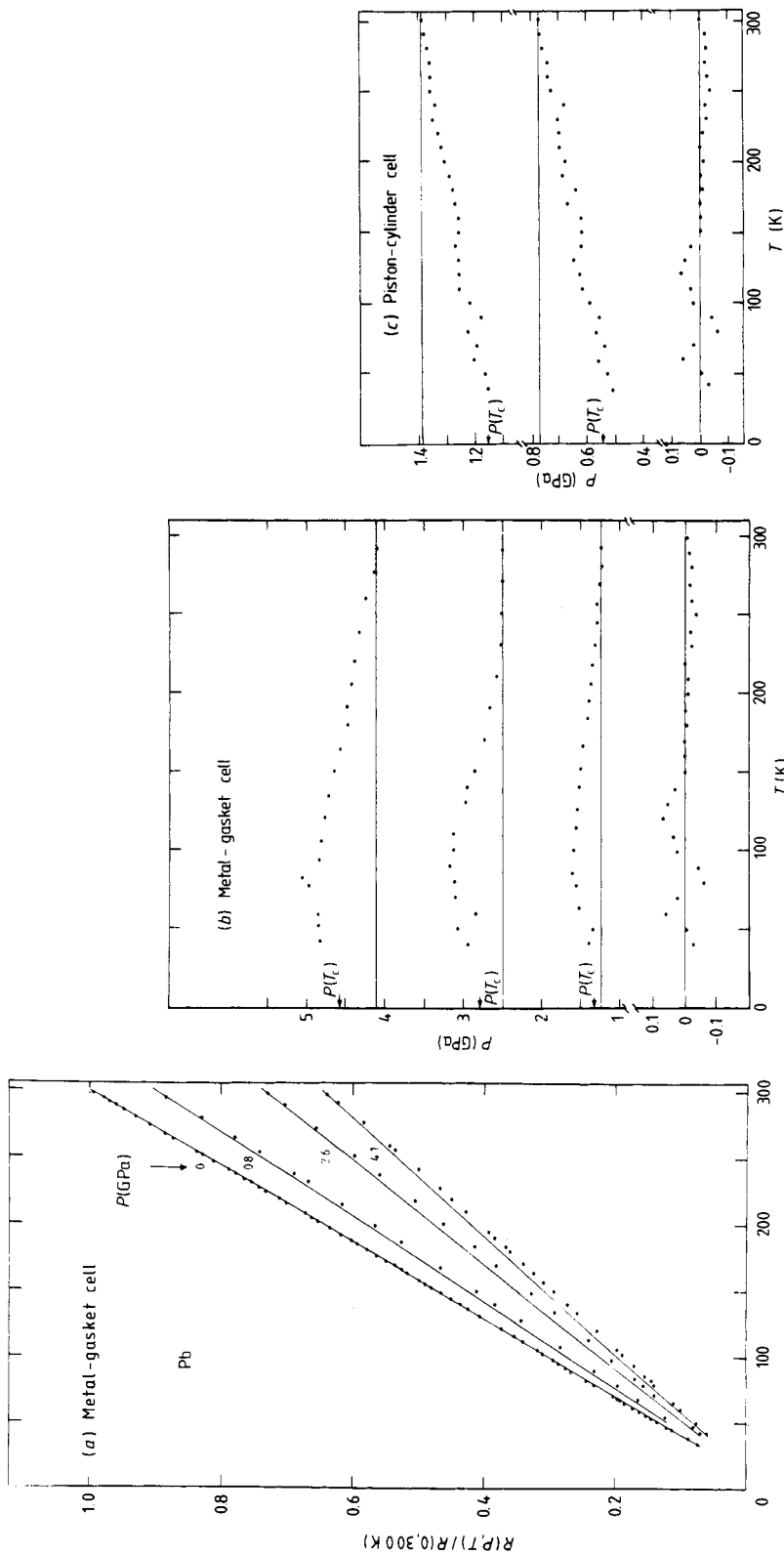

Figure 5. (*a*) Measured (O) and theoretical (——) temperature dependence of the relative resistance of Pb in metal-gasket cell at four pressures. (*b*) Pressure as a function of temperature derived from figure 5(*a*) using equation (9). $P(T_c)$ gives low-temperature pressure derived from the superconducting transition temperature of Pb. (*c*) Same as 5(*b*) except from data on Pb in a piston-cylinder cell.

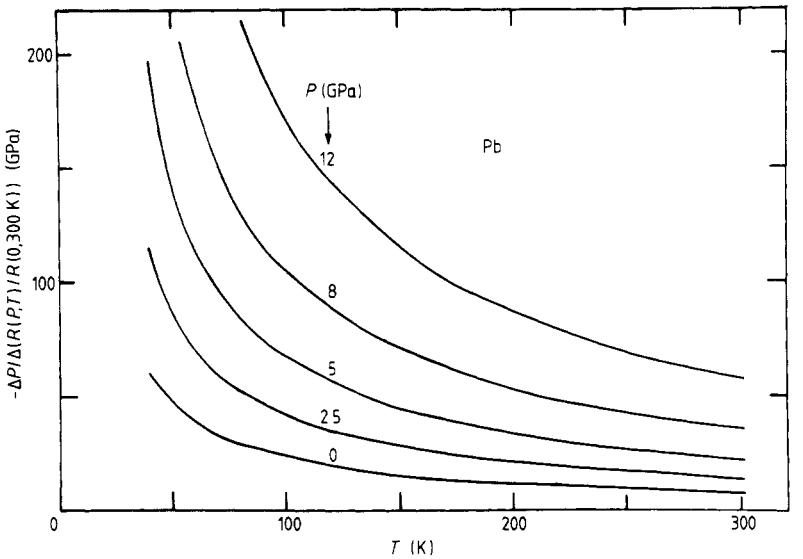

Figure 6. $(-\Delta P/\Delta R)$ for four different pressures from equation (5). Note the enhancement of $\Delta P/\Delta R$ at low temperatures which reduces the accuracy of the resistive manometer.

As a critical check on the accuracy of these resistive manometers it would be of interest to apply the above method to a pressure cell where changes of the opposite sign should occur. In fact, a pressure increase upon cooling is rather uncommon in hydrostatic high-pressure experiments. In the piston-cylinder technique it is normally believed (Becker and Hoo 1976) that pressure decreases upon cooling due to the rapid

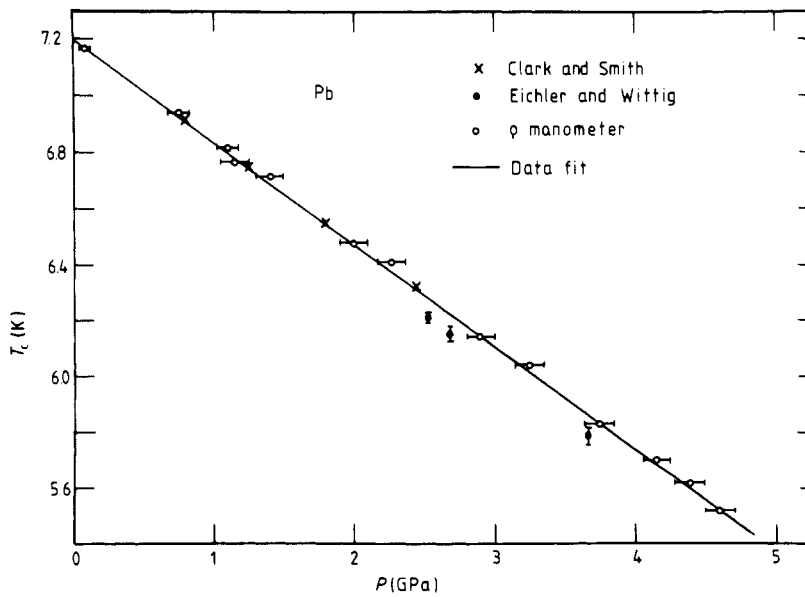

Figure 7. Pressure dependence of the superconducting transition of Pb from data by Clark and Smith (1978), Eichler and Wittig (1968), the present studies, and data fitted from equation (10).

Table 3. Calibration of In and Sn superconducting manometers. $T_c(P)$ of Pb manometer from figure 7.

P (GPa)	Pb T_c (K)	Sn T_c (K)	In T_c (K)
0	7.20	3.73	3.40
1.34	6.71	3.10	2.91
2.58	6.26	2.63	2.52
3.86	5.79	2.17	2.10
4.49	5.56	1.99	1.94

contraction of the pressure fluid. Unlike the metal-gasket cell, in the piston-cylinder technique most of the applied force is taken up by the pressure fluid itself. In figure 5(*c*) we show the temperature dependence of the pressure using a Pb resistive manometer in such a piston-cylinder cell (Peukert 1980). A decrease in pressure with temperature is actually observed. The indicated pressure decreases upon cooling approximately 0.2 GPa, and is only weakly dependent on pressure.

In figures 5(*b*) and (*c*) we compare the pressures given by the present resistive manometer to those from the superconducting Pb manometer calibrated by Clark and Smith (1978), and Eichler and Wittig (1968). The indicated pressures at low temperatures agree remarkably well! In numerous such comparisons we have found that the pressure difference using either manometer differs by less than ± 0.1 GPa. This excellent agreement supports the accuracy of not only the present resistive manometer but also of the superconducting manometers. In fact, we propose using the resistive manometer as a new method of calibrating T_c manometers (see figure 7). We note in passing that in experiments using quasi-hydrostatic pressure, where irreversible changes in sample length are unavoidable, a comparison of the resistive and superconducting manometers should allow an estimate of the sample elongation due to the expansion of the pressure cell and sample.

In addition to the development of the above resistive manometer, we have also calibrated the Pb, Sn and In superconducting manometers directly against one

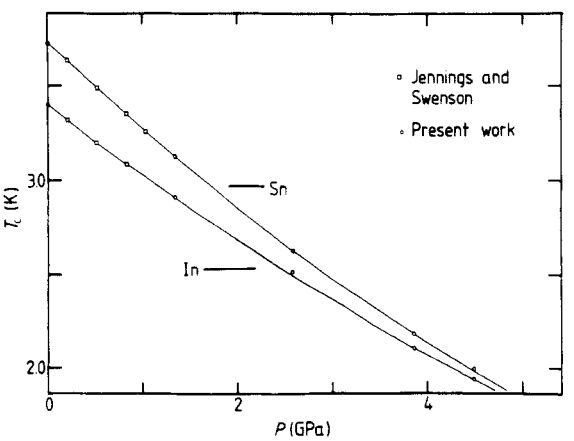

Figure 8. Pressure dependence of T_c of Sn and In from table 3. Full curve from equation (10).

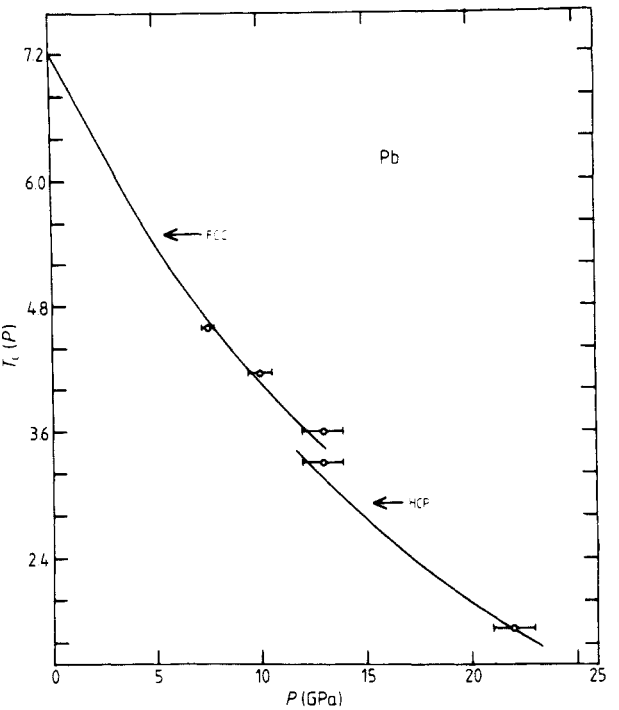

Figure 9. Pressure dependence of T_c of Pb to 5 GPa from figure 7, to 13 GPa corrected from Eichler and Wittig (1968), and at 22 GPa from Wittig *et al* (1979). The following calibration points (○) are used: Bi III–V 7.3 ± 0.2 GPa (Homan 1975), Pb I–II 13 ± 1 GPa (Decker *et al* 1972), GaP 22 ± 1 GPa (Piermarini and Block 1975). The volume decrease of Pb at the phase transition at 13 GPa is assumed to have a linear influence on T_c, resulting in the drop at 13 GPa.

another by incorporating all three simultaneously in miniature induction coils in a metal-gasket cell. We obtain the values of $T_c(P)$ given in table 3. In figure 8 these calibration points for Sn and In are compared to those of previous studies (Jennings and Swenson 1958). For convenience we list the following analytical expressions for $T_c(P)$ dependences to 5 GPa, giving the full curves in figures 7 and 8:

$$\begin{aligned} &\text{Pb} && T_c(P) = T_c(0) - (0.365 \pm 0.003)P \\ &\text{Sn} && T_c(P) = T_c(0) - (0.4823 \pm 0.002)P + (0.0207 \pm 0.0005)P^2 \\ &\text{In} && T_c(P) = T_c(0) - (0.3812 \pm 0.002)P + (0.0122 \pm 0.0004)P^2 \end{aligned} \tag{10}$$

where P is in GPa. For completeness we include in figure 9 a recent $T_c(P)$ calibration point for Pb of Wittig *et al* (1979) at 22 GPa. The $T_c(P)$ dependences given in figures 7, 8 and 9 are believed to represent the state of present knowledge.

3.3. Electron–phonon versus electron–electron scattering

The discussion up to now has been restricted to the simple Bloch–Grüneisen law (equation (1)) which consists exclusively of the contributions to the electrical resistivity from electron–phonon scattering processes. It can easily be shown (Ziman 1972) that $\rho_{BG} \propto T^1$ for $T \gg \theta$ and $\rho_{BG} \propto T^5$ for $T \ll \theta$ with temperature exponents between 5

and 1 in the intermediate temperature region. Inclusion of Umklapp processes in polyvalent metals such as Pb appears to only affect the temperature dependence of the resistivity in the intermediate region, the T^5 dependence at low temperatures persisting (Lawrence and Wilkins 1972).

A further contribution to the resistivity, that from electron–electron scattering, is characterised in the simplest approximation by

$$\rho_{ee} = \frac{K_e}{E_f}\left(\frac{T}{E_f}\right)^2 \tag{11}$$

(Ziman 1972), where K_e is analogous to K in equation (1). Electron–electron scattering has been observed in certain transition metals (Garland and Bowers 1968) at low temperatures. In simple polyvalent metals, however, ρ_{ee} is expected to be much weaker, being of importance only at the lowest temperatures ($T < 1$ K) (Lawrence and Wilkins 1973). The resistivity of ultra-pure Al was found by Van Kempen *et al* (1978) to be of the form $\rho = AT^2 + BT^5$ for $T \lesssim 2$ K, indicating the presence of both electron–electron and electron–phonon scattering contributions. To the authors' knowledge, no studies of comparable accuracy have been carried out on Pb. Van den Berg (1948) applied a magnetic field of 0.06 T to quench the superconductivity and found an approximate $\rho \propto T^5$ law for $T < 7$ K, this temperature exponent decreases progressively at higher temperatures. More accurate studies on Pb are necessary to test for a T^2 dependence at temperatures well below 7 K. In figure 10 are shown the results of the present measurements of the resistivity of Pb in the temperature range 7.2 K $\leqslant T \leqslant$ 17 K, to 4.4 GPa hydrostatic pressure. An approximate $T^{3.5}$ temperature

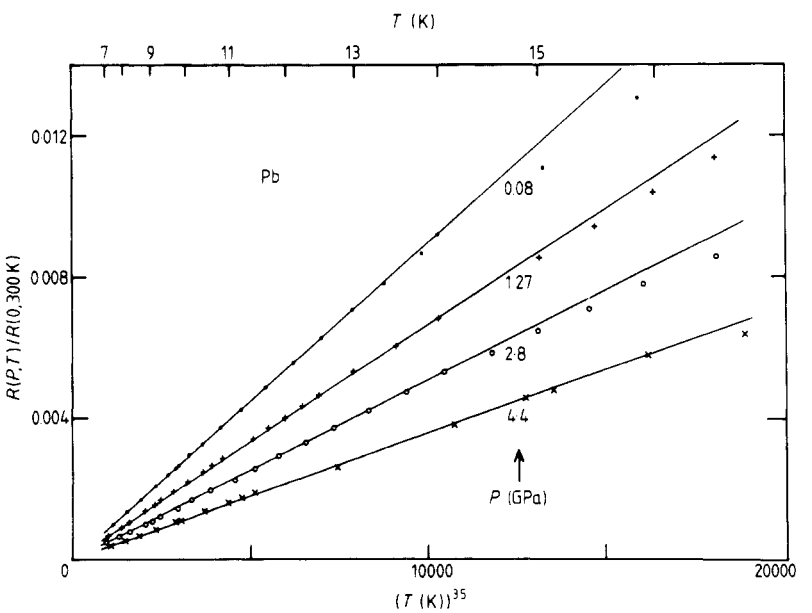

Figure 10. Resistance of Pb at various pressures versus $T^{3.5}$ relative to the value at 300 K and ambient pressure (21.1 μΩ cm, Landolt Börnstein 1960). Full lines drawn assuming the resistance to be proportional to $T^{3.5}$. The residual resistances have been subtracted off: 8 ± 2 nΩ cm at 0.08 GPa, 9 ± 2 nΩ cm at 1.27 GPa, 41 ± 3 nΩ cm at 2.8 GPa, 40 ± 2 nΩ cm at 4.4 GPa.

dependence is observed at all pressures; it is not possible to fit our data to a dependence like $\rho = AT^2 + BT^5$. The $T^{3.5}$ dependence is also consistent with the studies of Van den Berg (1948) in the same temperature range and thus presumably represents the approach to a T^5 dependence at temperatures below those of our studies. Over the temperature and pressure range considered, the temperature-dependent resistivity dominates the residual resistivity ρ_0 (see the caption to figure 10). Due to the sensitivity of ρ_0 to slight sample deformations, the intrinsic pressure dependence of ρ_0 could not be determined. It should be noted, however, that the pressure dependence of the $T^{3.5}$ slope is constant and does not reflect the jump in the value of ρ_0 between 1.27 GPa and 2.8 GPa.

We would like to propose here an alternative test for the presence of electron–electron scattering contributions; this method makes use of the fact that the electron–electron scattering has a relatively small pressure dependence. From equation (2) one has, neglecting the first term on the right-hand side of the equation, and assuming a power-law dependence $\rho_{BG} \propto T^n$, $\partial \ln \rho_{BG}/\partial \ln V = (n+1)\gamma$. In the same approximation, from equation (11), we obtain $\partial \ln \rho_{ee}/\partial \ln V = 3\gamma_e$, where $\gamma_e = -\partial \ln E_f/\partial \ln V = +2/3$ for a free-electron gas. Assuming for the moment ρ_{BG} has the same temperature dependence as ρ_{ee}, i.e. $\rho_{BG} \propto T^2$, then $\partial \ln \rho_{BG}/\partial \ln V = 3\gamma \simeq +8$ for Pb which lies well above the value $\partial \ln \rho_{ee}/\partial \ln V = 3\gamma_e = +2$. The latter result is shown by Kukkonen and Wilkins (1979) to hold to good accuracy not only in the Thomas–Fermi approximation but also in a more sophisticated theory where the interaction between two-electron quasi-particles is approximated in terms of the dielectric and vertex functions of the uniform electron gas. For a given temperature dependence, therefore, ρ_{BG} decreases much more rapidly with pressure than ρ_{ee}. This should be a useful method to establish in a given system whether or not an observed $\rho \propto T^2$ dependence originates from electron–electron or other scattering mechanisms.

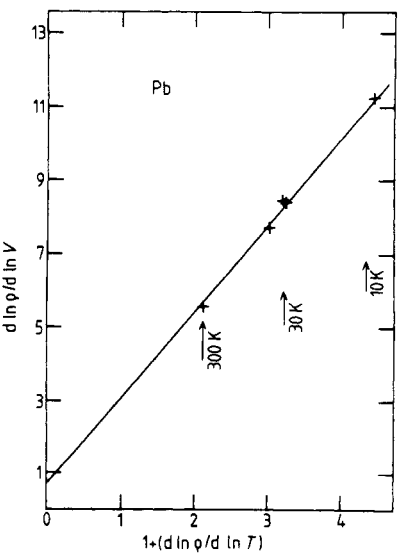

Figure 11. Measured volume derivative of the resistivity of Pb versus measured temperature derivative plotted according to equation (2). Linear dependence indicates dominance of electron–phonon scattering over the entire temperature range 7–300 K. The straight line is drawn for clarity.

Expressing this another way, if the electron–phonon mechanism dominates at all temperatures, then according to equation (2) a plot of $\partial \ln \rho / \partial \ln V$ versus $(1 + \partial \ln \rho / \partial \ln T)$ should give a straight line with slope γ and intercept $\partial \ln K / \partial \ln V$. In figure 11 we show such a plot using the data from figures 2, 3, 5 and 10. To show the accuracy of the data a straight-line dependence is indicated with intercept $\partial \ln K / \partial \ln V = +0.7$ and $\gamma = +2.5$. Our results support the dominance of electron–phonon scattering over the entire temperature range 7–300 K, as would be expected. To our knowledge, however, this method is new and could be used in both simple and transition metals as a test complementary to the $\rho \propto T^2$ dependence to help establish the presence or absence of electron–electron scattering. It is to be recognised, however, that in the temperature region where electron–electron scattering predominates over electron–phonon scattering, the residual scattering will in general be bigger still and its pressure dependence must be accurately known before our test could be applied.

We note that since the pressure method invokes only the volume dependence of the characteristic energies $k\theta$ or E_f, which can be determined in separate experiments, it would seem to be less model dependent than the $\rho \propto T^2$ test.

Acknowledgments

The authors would like to express their gratitude to S Methfessel for his support of this work.

References

Bassett W A and Takahashi T 1974 *Advances in High Pressure Research* vol 4, ed R H Wentorf Jr (New York: Academic) p 205

Becker W M and Hoo K 1976 *Rev. Sci. Instrum.* **47** 587–91

Birch F 1952 *J. Geophys. Research* **57** 240–68

Boehler R, Ramakrishnan J and Kennedy G C 1978 *Proc. 6th Conf. on AIRAPT* vol 2, ed K D Timmerhaus and M S Barber (New York: Plenum) pp 119–24

Bridgman P W 1970 *The Physics of High Pressure* (London: Dover)

Bundy F P and Strong H M 1962 *Solid State Phys.* **13** 81–146 (New York: Academic)

Clark M J and Smith T F 1978 *J. Low Temp. Phys.* **32** 495–503

Decker D L, Bassett W A, Merrill L, Hall H T and Barnett J D 1972 *J. Phys. Chem. Ref. Data* **1** 773–836

Dugdale J S 1969 *Advances in High Pressure Research* vol 2, ed R S Bradley (New York: Academic) pp 101–68

Eichler A and Wittig J 1968 *Z. Angew. Phys.* **25** 319–27

Eiling A and Schilling J S 1979 *Proc. 7th Conf. on AIRAPT* (New York: Pergamon) to be published

Fasol G and Schilling J S 1978 *Rev. Sci. Instrum.* **49** 1722–4

Garland J C and Bowers R 1968 *Phys. Rev. Lett.* **21** 1007–9

Gschneider K A 1964 *Solid State Phys.* **16** 275–426 (New York: Academic)

Homan C G 1975 *J. Phys. Chem. Solids* **36** 1249–54

Jennings L D and Swenson C A 1958 *Phys. Rev.* **112** 31–42

Kukkonen C A and Wilkins J W 1979 *Phys. Rev.* **19** 6075–93

Landolt Börnstein 1960 *Eigenschaften der Materie in ihren Aggregatzuständen* **6** *elektr. Eigenschaften* I pp 37, 80, 81

Lawrence W E and Wilkins J W 1972 *Phys. Rev.* B **6** 4466–82

——1973 *Phys. Rev.* B **7** 2317–32

Moore J P and Graves R S 1973 *J. Appl. Phys.* **44** 1174–8

Peukert H 1980 *Masters (Diplom) Thesis* University of Bochum

Piermarini G J and Block S 1975 *Rev. Sci. Instrum.* **46** 973–9
Piermarini G J, Forman R A and Block S 1978 *Proc. 6th Conf. on AIRAPT* (New York: Plenum) pp 860–4
Schilling J S, Ford P J, Larsen U and Mydosh J A 1976 *Phys. Rev.* B **14** 4368–80
Tomlinson P G and Carbotte J P 1977 *Can J. Phys.* **55** 751–60
Vaidya S N and Kennedy G C 1970 *J. Phys. Chem. Solids* **31** 2329–45
Van den Berg G J 1948 *Physica* **14** 111–38
Van Kempen H, Ribot H J M and Wyder P 1978 *J. Physique Coll.* **15** C6 1048–9
Washburn E W 1929 *Int. Critical Tables* vol 6 (New York: McGraw-Hill) p 129
Wittig J, Probst C, Schmidt F A and Gschneider Jr K A 1979 *Phys. Rev. Lett.* **42** 469–72
Zeto R J and Vanfleet H B 1969 *J. Appl. Phys.* **40** 2227–31
Ziman J M 1972 *Electrons and Phonons* (Oxford: Clarendon) pp 334–418
Zimmer F 1977 *PhD Thesis* University of Bochum